Detection of Temporary Lateral Confinement of Membrane Proteins Using Single-Particle Tracking Analysis

Rudolf Simson,* Erin D. Sheets,‡ and Ken Jacobson*§
*Department of Cell Biology and Anatomy, ‡Department of Chemistry, and §Lineberger Comprehensive Cancer Center, University of North Carolina at Chapel Hill, Chapel Hill, North Carolina 27599-7090 USA

ABSTRACT Techniques such as single-particle tracking allow the characterization of the movements of single or very few molecules. Features of the molecular trajectories, such as confined diffusion or directed transport, can reveal interesting biological interactions, but they can also arise from simple Brownian motion. Careful analysis of the data, therefore, is necessary to identify interesting effects from pure random movements. A method was developed to detect temporary confinement in the trajectories of membrane proteins that cannot be accounted for by Brownian motion. This analysis was applied to trajectories of two lipid-linked members of the immunoglobulin superfamily, Thy-1 and a neural cell adhesion molecule (NCAM 125), and the results were compared with those for simulated random walks. Approximately 28% of the trajectories for both proteins exhibited periods of transient confinement, which were <0.07% likely to arise from random movements. In contrast to these results, only 1.5% of the simulated trajectories showed confined periods. Transient confinement for both proteins lasted on average 8 s in regions that were ~280 nm in diameter.

INTRODUCTION

The development of nanovid microscopy and single-particle tracking (SPT) has made it possible to observe movements of single or small clusters of membrane proteins with nanometer level accuracy (Anderson et al., 1992; De Brabander et al., 1985; Fein et al., 1993; Geerts et al., 1987; Ghosh and Webb 1994; Sheetz et al., 1989). In SPT, proteins are labeled with antibody-coated colloidal gold particles or fluorescent latex beads, and their movements are followed using video-enhanced microscopy. According to the fluid mosaic model (Singer and Nicolson, 1972), proteins within the cell membrane are expected to undergo Brownian motion, which is best described as a random walk. Deviations from this expected behavior (e.g., the transient confinement of the protein to a small region) are interesting because they suggest interactions with other membrane constituents or peripheral structures. In this work, we report a method to detect transient confinement of membrane proteins in trajectories obtained by SPT. The analysis has been applied to two glycosylphosphatidylinositol (GPI)-anchored members of the immunoglobulin superfamily: Thy-1 and an isoform of the neural cell adhesion molecule, NCAM 125.

Confinement can be difficult to identify in a trajectory for two reasons. First, it may be of short duration and obscured by other parts of the trajectory. And second, Brownian diffusion can account for a wide variety of trajectory shapes that can temporarily mimic confinement (Berg, 1983; Rudnick and Gaspari, 1987). It is necessary, therefore, to establish criteria for distinguishing random behavior from true confinement. Following the work of Saxton (1993), we have developed a technique that allows the identification of periods of confined diffusion within a given trajectory and the exclusion of mimicked confinement.

MATERIALS AND METHODS

SPT experiments

NCAM 125 was observed in C2C12 mouse muscle cells; Thy-1 was observed in C3H $10T^1/_2$ fibroblasts. Data sets were recorded at a rate of 3 frames/s for 90 s for NCAM 125 and for 60 s for Thy-1, following Lee et al. (1991). These data will be fully described and interpreted in later publications.

Simulations of Brownian diffusion

Random walks (1100) were simulated for a range of diffusion coefficients D (1×10^{-11} cm^2/s $< D < 2 \times 10^{-10}$ cm^2/s), which is comparable with the diffusion coefficients for Thy-1 and NCAM 125. The jumpsize l was obtained for time $t = 0.003$ s, according to $l = (4Dt)^{1/2}$. For each jump, a random direction was chosen based on the random number generator *ran1* (Press et al., 1992), and 100 jumps were combined to form one step. Each simulated trajectory consisted of 300 frames (299 steps) and matches the recording rate of 3 frames/s used for NCAM 125 and Thy-1.

Analysis

To detect nonrandom confinement, we look for periods in which the protein remains in a membrane region for a duration considerably longer than a Brownian diffusant would stay in an equally sized region. Despite the fact that direction and size of every step of a random walk are unpredictable, it is possible to determine the probability ψ that a given

Received for publication 27 March 1995 and in final form 23 May 1995.

Address reprint requests to Dr. Ken Jacobson, Department of Cell Biology and Anatomy, University of North Carolina at Chapel Hill, Chapel Hill, NC 27599-7090. Tel.: 919-966-3855, 919-966-5703; Fax: 919-966-1856; E-mail: frap@med.unc.edu.

R. Simson's present address: Technical University Munich, Institute for Biophysics E22, 85748 Garching, Germany.

Abbreviations used: SPT, single-particle tracking; GPI, glycosylphosphatidylinositol; NCAM 125, neural cell adhesion molecule 125-kDa isoform.

0006-3495/95/09/989/05 $2.00

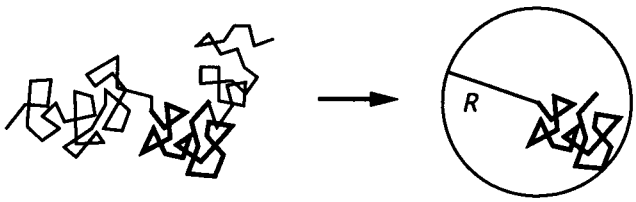

FIGURE 1 A short segment of a sample trajectory is tested for confinement. The radius R for a segment is determined by the point in the segment with the largest displacement from the starting point.

protein, with diffusion coefficient D, will stay in a region of radius R for a period of time t. By solving the diffusion equation for a point source at the origin and absorbing walls at R, Saxton (1993) determined this probability to be

$$\log \psi = 0.2048 - 2.5117\, Dt/R^2. \qquad (1)$$

For fixed R and D, ψ will decrease with increasing t because the likelihood of the particle reaching the wall and disappearing increases with time. Furthermore, for defined D and t, ψ increases with the size of the region R.

Because we do not know a priori the confinement conditions (i.e., when, how long, and how often a given particle will be confined during the observation time), we break the trajectory into shorter segments. Each segment contains a defined number of successive points of the trajectory. By assuming that the diffusion is Brownian, these segments can be treated as independent entities and Eq. 1 can be applied to each segment. The point within a segment with the largest displacement from the starting point determines the value of R for that segment (Fig. 1). The duration t of a segment, consisting of n frames, is given by $(n - 1)\Delta$, where Δ is the time between two recorded frames (here, $\Delta = 0.3$ s). D is approximated from the initial slope of the mean-squared displacement versus time plot for the entire trajectory (Lee et al., 1991). To accentuate regions of nonrandom behavior graphically, ψ is transformed into a probability level L according to Eq. 2:

$$L = \begin{cases} -\log(\psi) - 1 & \psi \le 0.1 \\ 0 & \psi > 0.1 \end{cases} \qquad (2)$$

For $\psi \ge 0$, L is always a positive number. If a segment has a likelihood $\ge 10\%$ to be of random origin ($\psi \ge 0.1$), it is assigned $L = 0$ because we are only interested in the detection of *nonrandom behavior*. The greater the tendency for nonrandom confinement (i.e., the smaller ψ is), the higher the value of L will be.

Every point within the trajectory is taken as starting point for a series of segments, ranging in size from 4 frames (3 steps) to a maximum segment size S_m (see Optimization of Parameters below). For each of these segments of varying length, L is calculated following Eq. 2. Because the segments overlap, each point within the trajectory will appear in a number of different segments. For every point within a trajectory, the probability levels L are averaged over all segments containing this specific point. Plotting the averaged L as a function of time yields a probability profile of the trajectory (Fig. 2). High values in the profile denote periods when the particle is confined to a region longer than a random diffusant would remain. A period of confined diffusion is defined by the position where the profile rises above a critical threshold level L_c for a duration $\tau \ge t_c$ (Fig. 2). We define τ as the duration of the confinement and the diameter of the circle circumscribing the corresponding segment of the trajectory as the size of the confinement zone.

Optimization of parameters

Because a random walk can temporarily mimic confinement, a probability profile for a random walk will not simply be a straight line (Fig. 2 *F*). However, the peaks in the profile arising from mimicked confinement are usually lower and narrower than peaks arising from nonrandom confinement (Fig. 2, *B* and *D*). To suppress the detection of mimicked confinement, the parameters t_c and L_c must be adjusted to values in which only minimal confined diffusion can be detected in profiles of Brownian trajectories, that is, the profile never rises above the level L_c for a period longer than t_c. So that true effects are not excluded, L_c and t_c should not be too high or long. For a given D, the value of L for a segment of duration t depends only on the radius R of that segment (see Eqs. 1 and 2). A short period of confinement within a large segment will not appreciably affect R for that segment. Thus, increasing the maximum segment size S_m smooths the profile because the probability levels will now be averaged over larger segments of the trajectory, thereby succeeding in suppressing the shorter lived mimicked confinement of Brownian motion (Fig. 3). If S_m is too high,

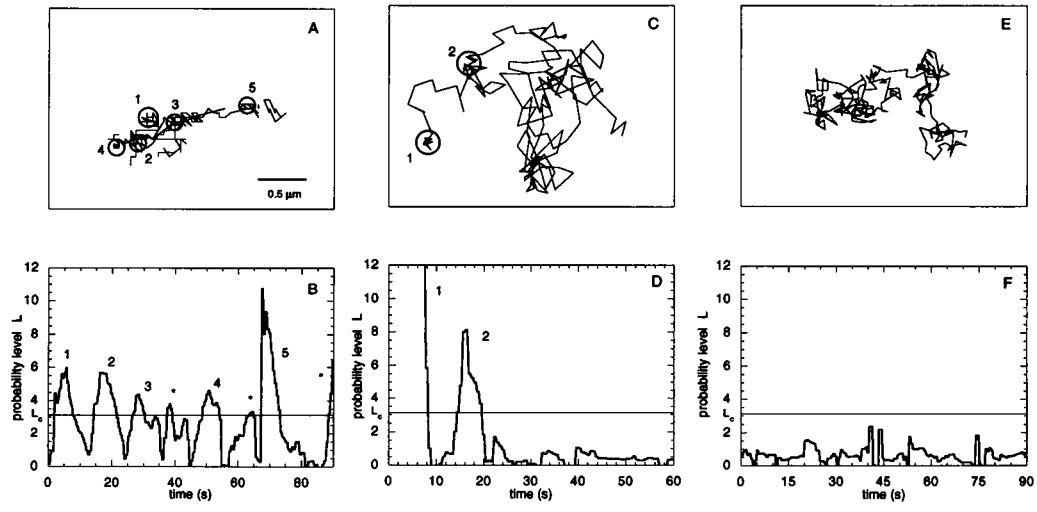

FIGURE 2 Temporary confinement in a trajectory is denoted by regions of the profile that rise above the critical threshold level $L_c = 3.16$ for longer than $t_c = 2.7$ s. Shown are examples of trajectories and probability profiles for NCAM 125 in C2C12 muscle cells (*A*, *B*), Thy-1 in C3H $10T^1/_2$ fibroblasts (*C*, *D*), and simulated Brownian diffusion (*E*, *F*). Confinement zones (circled) and their corresponding peaks in the profile are numbered in the order of their appearance. Note that there is a significant difference between the profiles for the protein trajectories (*B*, *D*) and the profile for a random walk (*F*). The three peaks (*) in profile *B* are not confinement zones because they rise above L_c for a period $\tau < t_c$. Peak 1 in profile *D* reaches a level of $L = 60$, corresponding to a likelihood of $1 \times 10^{-59}\%$ of being of random origin. Note that the trajectories are drawn to the same scale.

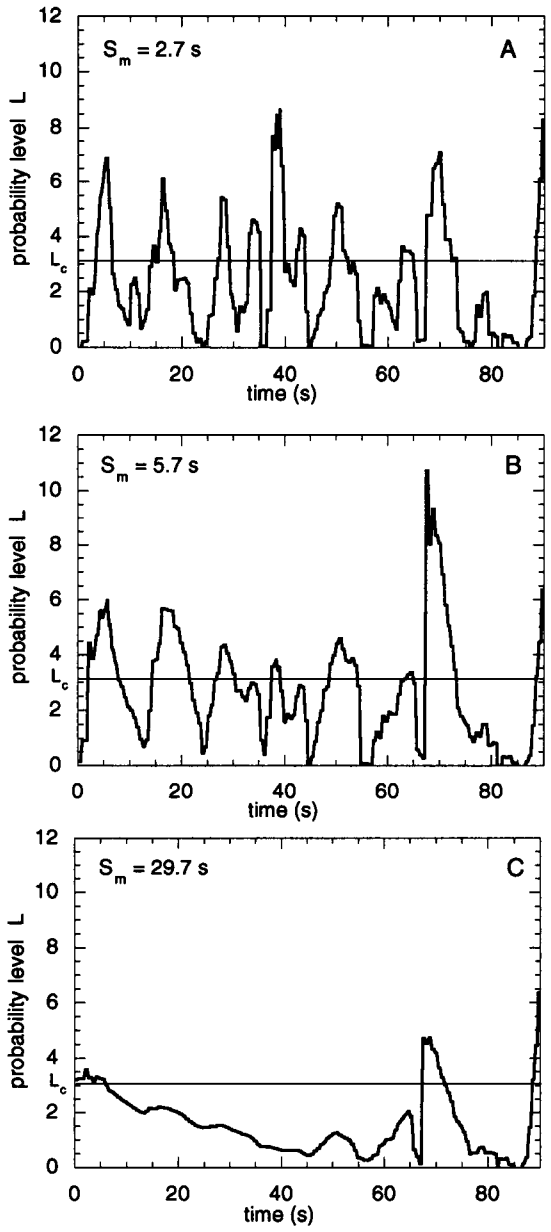

FIGURE 3 Probability profiles were calculated for the NCAM trajectory shown in Fig. 2 *A* using different values of S_m. Note that if S_m is too low, noise from the random distribution of step sizes is observed in the profile (*A*). When S_m is too large, information about possible confinement is lost (*C*). Shown are S_m = 2.7 s (*A*), S_m = 5.7 s (*B*), and S_m = 29.7 s (*C*).

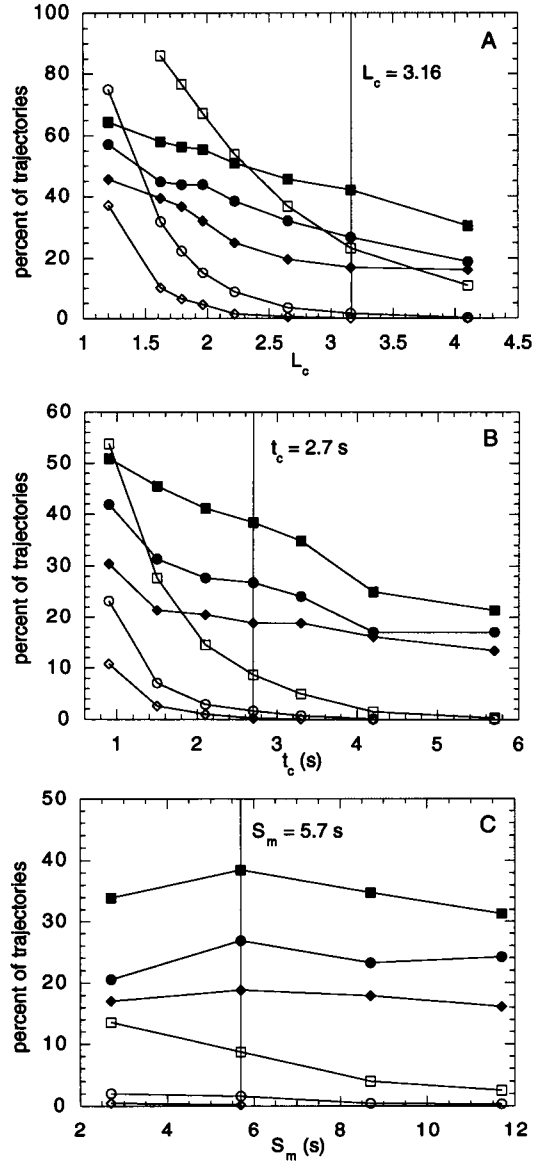

FIGURE 4 The percentages of trajectories exhibiting confined diffusion were plotted against the values of L_c (*A*), t_c (*B*), and S_m (*C*) that were used for calculating the probability profile. Shown are the results for simulations (*empty markers*) and NCAM 125 (*filled markers*). The vertical lines show the values used in setting 1 (Table 1). (*A*) Shown is the influence of L_c when S_m = 5.7 s. Different values of t_c were used (t_c = 0.9 s, *squares*; t_c = 2.7 s, *circles*; t_c = 4.2 s, *diamonds*). (*B*) Shown is the influence of t_c when S_m = 5.7 s. Different threshold values L_c were used (L_c = 2.22, *squares*; L_c = 3.16, *circles*; L_c = 4.10, *diamonds*). (*C*) Shown is the influence of S_m when t_c = 2.7 s. Different threshold values L_c were used (L_c = 2.22, *squares*; L_c = 3.16, *circles*; L_c = 4.10, *diamonds*).

however, structure in the profile resulting from nonrandom confinement may be suppressed as well (Fig. 3 *C*). Therefore, the value of S_m must be optimized for minimizing detection of confinement in the simulated trajectories and maximizing detection in the protein trajectories. The effects of different parameter settings on the detection of confined diffusion in both experimental and simulated data were examined (Fig. 4). From these results, the settings L_c = 3.16, t_c = 2.7 s, and S_m = 5.7 s were chosen. Note that the threshold L_c = 3.16 is <0.07% likely to have a random origin.

RESULTS AND DISCUSSION

We compared the behavior of two membrane proteins, NCAM 125 and Thy-1, with simulated random walks. Apparent confinement, arising from Brownian motion, usually yields narrow and low peaks in the probability profile (Fig. 2 *F*). With the appropriate profile settings (L_c = 3.16, t_c = 2.7 s, S_m = 5.7 s), we could successfully minimize the detection of these mimicked confinement zones and still identify a significant amount of temporary confinement in the protein trajectories (Fig. 4; Table 1). Profile peaks in NCAM 125 and Thy-1 could reach probability levels of $L \geq$

TABLE 1 Confinement zones detected in protein trajectories and simulated random walks for different profile settings

	Trajectories with conf. zones. (%)	Number of conf. zones*	Diameter of conf. zones* ± SD (nm)	Duration of conf. zones* ± SD (s)
NCAM 125 (n = 112)				
Setting 1‡	27	2	280 ± 160	7.2 ± 4.5
Setting 2§	32	2	228 ± 116	5.6 ± 4.3
Setting 3¶	40	2	386 ± 164	6.4 ± 3.4
Thy-1 (n = 63)				
Setting 1	29	2	274 ± 176	7.8 ± 5.6
Setting 2	32	2	249 ± 164	6.8 ± 5.7
Setting 3	33	2	304 ± 158	8.9 ± 5.5
Simulations (n = 1100)				
Setting 1	1.5	1	270 ± 196	3.1 ± 0.2
Setting 2	6.0	1	160 ± 104	1.9 ± 0.4
Setting 3	8.4	1	280 ± 222	3.4 ± 0.7

* Results are averaged over trajectories containing at least one confinement zone.
‡ Setting 1: L_c = 3.16, t_c = 2.7 s, S_m = 5.7 s.
§ Setting 2: L_c = 3.16, t_c = 1.2 s, S_m = 5.7 s.
¶ Setting 3: L_c = 2.22, t_c = 2.7 s, S_m = 5.7 s.

20, with the corresponding confinement zones having a probability $\leq 1 \times 10^{-19}$% of being of random origin. For NCAM 125, observed for 90 s, we found periods of confined diffusion in 27% of the trajectories. As many as five different confinement zones, which were ~280 nm in diameter and lasted on average 7.2 s, were observed in a single trajectory (Table 1). Similar results were obtained for Thy-1, which was observed for 60 s. Here 29% of the trajectories contained one to four confined periods lasting ~7.8 s/duration. These regions were ≈274 nm in diameter (Table 1). With the same profile settings, we detected nonrandom confinement in 1.5% of the simulated random walks. Those trajectories contained only one or two confinement periods that existed for 3.1 s, on average. For the simulated data, the average size of confinement zones is largely determined by the value of t_c (Table 1). For NCAM 125 and Thy-1, however, the average duration and diameter of the confinement zones demonstrated little dependence upon different profile settings (Table 1). Decreasing the value of L_c or t_c leads to detection of confined diffusion in an increasing number of trajectories (Fig. 4, *A* and *B*; Table 1). Increasing S_m suppresses the detection of confinement in simulated random walks while minimally affecting the probability profiles of the protein trajectories (Fig. 4 *C*).

The probability profile described here is a practical and convenient method for detecting temporary confinement that cannot be accounted for by the family of random walks. Confinement represents a departure from the free, unrestricted lateral diffusion predicted by the fluid mosaic model (Singer and Nicolson, 1972) and, therefore, may be an important facet of the dynamic structure of membranes. Several recent studies have reported temporarily confined diffusion for a variety of membrane-spanning proteins. The observed confinement (in regions 300–400 nm in diameter) was attributed to interactions between the cytoplasmic protein domains with the membrane-apposed cytoskeleton (Anderson et al., 1992; Edidin et al., 1991; 1994; Kusumi et al., 1993; Sako and Kusumi, 1994). However, the applications presented here show that transient confinement also occurs for GPI-anchored proteins. This result is intriguing because interactions between the protein and the cytoskeletal meshwork are impossible without invoking a third party. Obstacles on the cell surface, possibly linked to the cytoskeleton or interactions within the lipid bilayer, could temporarily confine the protein to small regions (Saxton, 1994; Sheets et al., 1995; Simson et al., 1995). However, the exact mechanism and the biological implications of confinement remain to be explored.

The C2C12 mouse muscle cells that were transfected with human NCAM 125 were kindly provided by Dr. Frank Walsh (Guy's Hospital, London). Some of the measurements on Thy-1 were performed by Dr. Greta Lee (University of North Carolina). We thank Drs. Michael Saxton (University of California, Davis) and Greta Lee for helpful discussions.

This work was supported by National Institutes of Health grant GM 41402.

REFERENCES

Anderson, C. M., G. N. Georgiou, I. E. G. Morrison, G. V. W. Stevenson, and R. J. Cherry. 1992. Tracking of cell surface receptors by fluorescence digital imaging microscopy using a charge-coupled device camera. Low-density lipoprotein and influenza virus receptor mobility at 4°C. *J. Cell Sci.* 101:415–425.

Berg, H. C. 1983. Random Walks in Biology. Princeton University Press, Princeton, NJ. 11–12.

De Brabander, M., S. Geuens, R. Nuydens, M. Moeremans, and J. De Mey. 1985. Probing microtubule-dependent intracellular mobility with nanometre particle video ultramicroscopy (nanovid ultramicroscopy). *Cytobios.* 43:273–283.

Edidin, M., S. C. Kuo, and M. P. Sheetz. 1991. Lateral movements of membrane glycoproteins restricted by dynamic cytoplasmic barriers. *Science.* 254:1379–1382.

Edidin, M., M. C. Zúñiga, and M. P. Sheetz. 1994. Truncation mutants define and locate cytoplasmic barriers to lateral mobility of membrane glycoproteins. *Proc. Natl. Acad. Sci. USA.* 91:3378–3382.

Fein, M., J. Unkeless, F. Y. S. Chuang, M. Sassaroli, R. da Costa, H. Väänänen, and J. Eisinger. 1993. Lateral mobility of lipid analogues and GPI-anchored proteins in supported bilayers determined by fluorescent bead tracking. *J. Membr. Biol.* 135:83–92.

Geerts, H., M. De Brabander, R. Nuydens, S. Geuens, M. Moeremans, J. De Mey, and P. Hollenbeck. 1987. Nanovid tracking: a new automatic method for the study of mobility in living cells based on colloidal gold and video microscopy. *Biophys. J.* 52:775–782.

Ghosh, R. N., and W. W. Webb. 1994. Automated detection and tracking of individual and clustered cell surface low density lipoprotein receptor molecules. *Biophys. J.* 66:1301–1318.

Kusumi, A., Y. Sako, and M. Yamamoto. 1993. Confined lateral diffusion of membrane receptors as studied by single particle tracking (nanovid microscopy). Effects of calcium-induced differentiation in cultured epithelial cells. *Biophys. J.* 65:2021–2040.

Lee, G. M., A. Ishihara, and K. A. Jacobson. 1991. Direct observation of Brownian motion of lipids in a membrane. *Proc. Natl. Acad. Sci. USA.* 88:6274–6278.

Press, W. H., S. A. Teukolsky, W. T. Vetterling, and B. P. Flannery. 1992. Numerical Recipes in C, 2nd ed. Cambridge University Press, New York. 280 pp.

Rudnick, J., and G. Gaspari. 1987. The shapes of random walks. *Science.* 237:384–389.

Sako, Y., and A. Kusumi. 1994. Compartmentalized structure of the plasma membrane for receptor movements as revealed by a nanometer-level motion analysis. *J. Cell Biol.* 125:1251–1264.

Saxton, M. J. 1993. Lateral diffusion in an archipelago: single-particle diffusion. *Biophys. J.* 64:1766–1780.

Saxton, M. J. 1994. Anomalous diffusion due to obstacles: a Monte Carlo study. *Biophys. J.* 66:394–401.

Sheets, E. D., G. M. Lee, and K. Jacobson. 1995. Mechanisms for immobilization of a GPI-linked protein using single particle tracking analysis. *Biophys. J.* 68:306*a*. (Abstr.)

Sheetz, M. P., S. Turney, H. Qian, and E. L. Elson. 1989. Nanometre-level analysis demonstrates that lipid flow does not drive membrane glycoprotein movements. *Nature.* 340:284–288.

Simson, R., B. Yang, P. Doherty, S. Moore, F. Walsh, and K. Jacobson. 1995. The mosaic structure of cell membranes revealed by transient confinement of GPI-linked NCAM-125. *Biophys. J.* 68:436*a*. (Abstr.)

Singer, S. J., and G. L. Nicolson. 1972. The fluid mosaic model of the structure of cell membranes. *Science.* 175:720–731.